

Exotic states of matter with polariton chains

Kirill Kalinin¹, Pavlos G. Lagoudakis^{1,2} and Natalia G. Berloff^{1,3*}

¹*Skolkovo Institute of Science and Technology Novaya St.,
100, Skolkovo 143025, Russian Federation*

²*Department of Physics and Astronomy, University of Southampton,
Southampton, SO17 1BJ, United Kingdom and*

³*Department of Applied Mathematics and Theoretical Physics,
University of Cambridge, Cambridge CB3 0WA, United Kingdom*

(Dated: October 9, 2017)

Abstract

We consider linear periodic chains of exciton-polariton condensates formed by pumping polaritons non-resonantly into a linear network. To the leading order such a sequence of condensates establishes relative phases as to minimize a classical one-dimensional XY Hamiltonian with nearest and next to nearest neighbours. We show that the low energy states of polaritonic linear chains demonstrate various classical regimes: ferromagnetic, antiferromagnetic and frustrated spiral phases, where quantum or thermal fluctuations are expected to give rise to a spin liquid state. At the same time nonlinear interactions at higher pumping intensities bring about phase chaos and novel exotic phases.

*correspondence address: N.G.Berloff@damtp.cam.ac.uk

Frustrated spin systems represent one of the most demanding problems of condensed matter physics [1, 2]. Various strongly correlated states are realised by Hubbard models [3, 4], that, in particular limits, reduce to spin models. Geometric frustration leads to a rich variety of possible spin configurations in the ground and excited states of these systems due to the competition between interactions and the geometry of the spin lattice with a potential of creating novel, exotic classical and quantum phases, such as resonating valence bond states and valence bond solids, as well as various kinds of quantum, topological and critical spin liquids [5, 6]. A spin liquid is a much sought state of matter with applications to high-temperature superconductivity and quantum computation. In this state, spins fluctuate in a liquid form without ever solidifying even in the ground state [7]. In real systems, the classical spin Heisenberg Hamiltonians are at best approximate. The real Hamiltonians are affected by assorted perturbations such as quantum and thermal fluctuations, anisotropies, disorder, dipolar interactions, coupling to lattice degrees of freedom. Depending on interactions and connectivity classical Heisenberg models may exhibit frustration with a large ground state degeneracy. The ground state manifold has no energy scale of its own and therefore such perturbations may bring about unusual disordered spin liquid, Bose metal states with exotic excitations and novel phase transitions. The theoretical possibility of quantum fluctuations combined with geometric spin frustration has been hotly debated since Anderson proposed them in 1973 [8] and only recently have been realised experimentally [9]. It remains to be seen which exotic phases other types of perturbations can produce. This can be elucidated by studying emergence phenomena: the dynamical generation of new types of degrees of freedom using some condensed matter systems to mimic (simulate) spontaneously and collectively different ones, possibly unknown or otherwise unrealizable.

Various systems have been proposed to act as analog classical or quantum simulators to mimic condensed matter phenomena and realise disparate kinds of spin models: ultracold atomic and molecular gases in optical lattices [10–13], defects and vacancies in semiconductors or dielectric materials [14, 15], magnetic impurities embedded in solid helium [16], photons [17], trapped ions [18, 19], superconducting q-bits [20], network of optical parametric oscillators (OPOs) [21, 22], coupled lasers [23].

Recently, we introduced polariton graphs as a new platform to study unconventional superfluids, spin liquids, and many other systems based on the XY Hamiltonian [24]. Polariton condensates can be imprinted into any two-dimensional graph by spatial modulation

of the pumping laser [25] and can be easily scalable to a large number of lattice sites. In the regime of non-resonant excitation, the individual condensates in a polariton graph select their relative phases without the influence of the pumping laser. The condensation is driven by bosonic stimulation, so that polariton graph condenses at the state with the phase-configuration that carries the highest polariton occupancy [26], which corresponds to the global minimum of the XY Hamiltonian. The structure of the XY Hamiltonian is set by the interaction strengths among the condensates that are defined by the systems parameters such as the graph geometry, the pumping profile and intensity. The XY model is a mathematical abstraction of spin system such as a disordered magnetic material composed of competitively interacting spins. For such a system, a spin indexed by i is represented by a two-dimensional unit vector $\mathbf{s}_i = (\cos \theta_i, \sin \theta_i)$, the energy is expressed by the XY Hamiltonian $H_{XY} = -\sum_{i<j} J_{ij} \mathbf{s}_i \cdot \mathbf{s}_j = -\sum_{i<j} J_{ij} \cos(\theta_i - \theta_j)$, where J_{ij} denotes the coupling coefficient between the i th and j th spins. We refer to the coupling as ferromagnetic (antiferromagnetic) if $J_{ij} > 0$ ($J_{ij} < 0$). The XY model is a limiting case of the Heisenberg spin model or n -vector model for $n = 2$. The vectors correspond to the directions of spins (originally quantum mechanical) in a material in which the z -component of spins couples less than the x and y components. Since H_{XY} is the simplest model that undergoes the $U(1)$ symmetry-breaking transition, it has been discussed in the connection to classical magnetic systems, unconventional superfluid, topological quantum information processing and storage, quantum phase transitions, spin-liquid and spin-ice phases and high- T_c superconductivity.

In this letter, we propose to exploit the properties of polariton graphs to generate various frustrated states and spinor phases. In particular, we show that at the condensation threshold depending on the structure of the corresponding XY Hamiltonian the polariton condensates establish the relative phases that correspond to the classical ferromagnetic, antiferromagnetic, frustrated states as well as the novel exotic states that can be associated with a spin wave, spin liquid, phase chaos and cross-breeds between them.

The theoretical approach, presented here, is based on the well-known complex Ginzburg-Landau equation (cGLE) with a saturable nonlinearity [27, 28], that was successfully used for the modelling of polariton condensates. Written for the condensate wavefunction ψ in

one-dimension, cGLE reads as

$$i\hbar \frac{\partial \psi}{\partial t} = -\frac{\hbar^2}{2m} (1 - i\eta_d N_R) \psi_{xx} + U_0 |\psi|^2 \psi + \hbar g_R N_R(x) \psi + \frac{i\hbar}{2} (R_R N_R(x) - \gamma_C) \psi, \quad (1)$$

where $N_R = P(x)/(\gamma_R + R_R |\psi|^2)$ is the density of the hot exciton reservoir, m is polariton effective mass, U_0 and g_R are the strengths of effective polariton-polariton and polariton-exciton interactions, respectively, η_d is the energy relaxation coefficient specifying the rate at which gain decreases with increasing energy, R_R is the rate at which the reservoir excitons enter the condensate, γ_C and γ_R are the rates of the condensate polaritons and reservoir excitons losses, respectively, and P is the pumping into the reservoir. When pumped into several spots with the outflows from each spot reaching its neighbours the system establishes a global coherence with a chemical potential μ if the characteristics of the pump (intensity, spatial shape) are not vastly different from one spot to another. The steady state of such system satisfies

$$\mu \Psi = -(1 - i\eta n) \Psi_{xx} + |\Psi|^2 \Psi + g n(x) \Psi + i(n(x) - \gamma) \Psi, \quad (2)$$

$$n = \frac{p(x)}{(1 + b|\Psi|^2)}, \quad (3)$$

where we non-dimensionalized Eq. (1) using $\psi \rightarrow \sqrt{\hbar^2/2mU_0 l^2} \Psi$, $\mathbf{r} \rightarrow l\mathbf{r}$, $t \rightarrow 2mtl^2/\hbar$ and introducing the notations $g = 2g_R/R_R$, $\gamma = m\gamma_C l^2/\hbar$, $p = ml^2 R_R P(\mathbf{r})/\hbar\gamma_R$, $\eta = \eta_d \hbar/mR_R l^2$, and $b = R_R \hbar^2/2ml^2 \gamma_R U_0$. We choose the unit length as $l = 1\mu m$. The Madelung transformation $\Psi = \sqrt{\rho} \exp[iS]$ relates the wavefunction to density $\rho = |\Psi|^2$ and velocity $u = S_x$. To derive the coupling strength we consider a single pumping spot centered at the origin and exponentially decaying to zero away from it. At large x , where $p(x) = 0$, the velocity u is given by the outflow wavenumber $k_c = const$ with $\rho_x/\rho = -\gamma/k_c$, which can be integrated to yield $\rho \sim \exp[-x\gamma/k_c]$. From Eq. (2), therefore, we obtain $\mu = k_c^2 - \gamma^2/4k_c^2$ at infinity.

The wave function, that approximately describes the system of ℓ identical pumping spots at positions x_i , takes the form $\Psi_g(x) \approx \sum_{i=1}^{\ell} \Psi_i(x - x_i)$, where the wave function of a single pumping spot centred at $x = x_i$ can be approximated by $\Psi_i(x - x_i) = \sqrt{\rho(x - x_i)} \exp[(ik_c|x - x_i|) + i\theta_i]$, where θ_i is a space independent part of the phase. In the expression for the space varying phase we neglected the healing of the outflow velocity to zero at the center of the

pump. This healing occurs on the lengthscale of the order of the width of the pump and can be neglected when evaluating the integral quantities over the entire sample. We note that nonlinearity of the system affects the assumption of the linear superposition of the individual wavefunctions in several ways: not only it rescales the single wavefunction in the superposition and decreases the chemical potential of the superposition in the steady state, but also for small distances between the pumping spots may bring about periodic and disordered fluctuations of the phase differences between the condensates. However, for well separated condensates this approximation is valid.

Depending on the pumping parameters, the system will lock with the relative phases $\theta_{ij} \equiv \theta_i - \theta_j$ between the sites i and j to achieve the highest occupation number – the total amount of matter given by $\mathcal{D} = \int_{-\infty}^{\infty} |\Psi_g|^2 dx$ [26]. To evaluate \mathcal{D} we work in the Fourier space and write

$$\begin{aligned} \mathcal{D} &= \frac{1}{2\pi} \int |\widehat{\Psi}_g(k)|^2 dk \approx \frac{1}{2\pi} \int \left| \sum_i \widehat{\Psi}_i(k) \right|^2 dk = \\ &= \ell \mathcal{D}_0 + \frac{1}{\pi} \sum_{i < j} \int \left(\widehat{\Psi}_i \widehat{\Psi}_j^* + c.c. \right) dk \end{aligned} \quad (4)$$

where \mathcal{D}_0 is the number of particles of a single isolated condensate, $\widehat{\Psi}_g(k)$ is the Fourier transform of Ψ_g , and

$$\begin{aligned} \widehat{\Psi}_i(k) &= \int_{-\infty}^{\infty} \Psi_i(x - x_i) \exp(-ikx) dx = \\ &= \exp(-ikx_i) \int_{-\infty}^{\infty} \Psi_i(\alpha) \exp(-ik\alpha) d\alpha = \\ &= \exp(-ikx_i + i\theta_i) \widehat{\psi}(k), \end{aligned} \quad (5)$$

$$\widehat{\psi}(k) = 2 \int_0^{\infty} \sqrt{\rho(\alpha)} \exp(ik_c \alpha) \cos(k\alpha) d\alpha. \quad (6)$$

Denoting the distances between the spots as $x_{ij} = x_i - x_j$ we substitute (5) into the integral in Eq. (4) to get:

$$\mathcal{D} = \ell \mathcal{D}_0 + \frac{2}{\pi} \sum_{i < j} \cos \theta_{ij} \int_0^{\infty} |\widehat{\psi}(k)|^2 \cos(kx_{ij}) dk. \quad (7)$$

This implies that during the condensation the system of pumping spots establishes the phase

difference in such a way as to minimize \mathcal{H}_{XY} , where the coupling strengths are given by

$$J_{ij} = \frac{2}{\pi} \int_0^\infty |\widehat{\psi}(k)|^2 \cos(kx_{ij}) dk. \quad (8)$$

To obtain an analytical approximation of the coupling strengths and a criterion for the switching between the ferro- and antiferromagnetic connections along the chain of pumped condensate, we parameterise the amplitude of the condensate by the inverse width β and the height A : $\sqrt{\rho(x)} \approx A \exp[-\beta|x|]$. We expect the width and the height of the condensate to correlate with the width and the intensity of the pumping profile, respectively. For this approximation of the amplitude the integrals in Eqs. (7) and (8) can be evaluated exactly.

$$\begin{aligned} \widehat{\psi}(k) &= 2A \int_0^\infty \exp(-\beta\alpha + ik_c\alpha) \cos(k\alpha) d\alpha \\ &= \frac{2A(\beta - ik_c)}{\beta^2 + k^2 - 2i\beta k_c - k_c^2}. \end{aligned} \quad (9)$$

$$J_{ij} = \frac{8A^2}{\pi} \int_0^\infty \frac{(\beta^2 + k_c^2) \cos(kx_{ij}) dk}{\beta^4 + (k^2 - k_c^2)^2 + 2\beta^2(k^2 + k_c^2)}. \quad (10)$$

Applying the residue theorem for evaluating the last integral, we obtain the closed form expression for the coupling constants

$$J_{ij} = 2A^2 \left[\frac{1}{\beta} \cos(k_c x_{ij}) + \frac{1}{k_c} \sin(k_c x_{ij}) \right] e^{-\beta x_{ij}}. \quad (11)$$

This expression determines the switching of ferro- and antiferromagnetic coupling between the neighbours since the sign of J_{ij} is set by the expression $\cos(k_c x_{ij})/\beta + \sin(k_c x_{ij})/k_c$. If the pumping profile is wide (β is small), the sign of the interactions is determined by $\cos(k_c x_{ij})$, which is what we expect directly from Eq. (8) since $|\widehat{\psi}(k)|^2 \sim \delta(k - k_c)$ for a wide pumping spot.

Now we consider a linear periodic chain of ℓ equidistant polariton condensates separated by $x_{ij} = d$. This chain can be achieved by creating a sequence of trapped condensates [29, 30] or by pumping condensates around a circle [24, 31]. The corresponding XY model takes form $\mathcal{H} = -J_1 \sum_i \mathbf{s}_i \cdot \mathbf{s}_{i+1} - J_2 \sum_i \mathbf{s}_i \cdot \mathbf{s}_{i+2}$, where the sum is over all ℓ condensates with periodic boundary conditions. In case of $J_2 = 0$ the model is integrable [32], whereas for $J_2 \neq 0$ the exact solutions were found for a limited set of values of J_2/J_1 . Frustrated

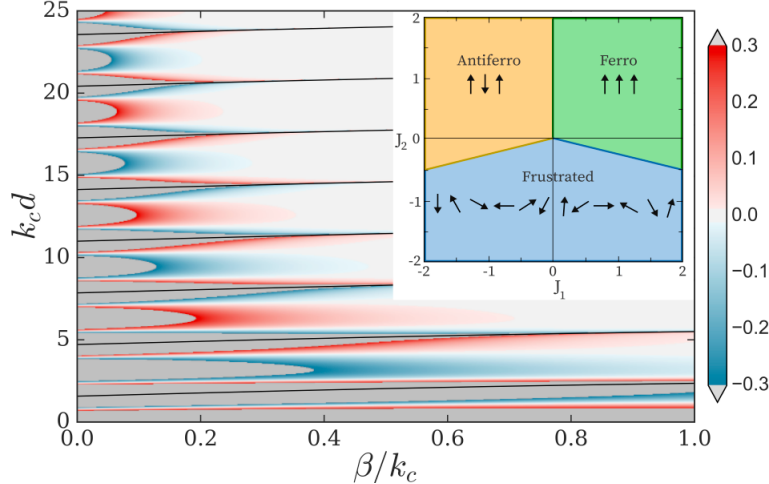


FIG. 1: Contour plot of frustration parameter J_2/J_1 as a function of $k_c d$ and β/k_c , where k_c is the polariton outflow wavevector, β is the inverse width of the polariton spot, d is the distance between the two adjacent spots. The coupling strengths J_1 and J_2 are calculated from Eq. (11) for the distances d and $2d$, respectively. The sign changes for J_1 are shown by black solid lines. The inset shows the different regimes of classical XY model on the $J_2 - J_1$ plane: ferromagnetic, antiferromagnetic and frustrated.

phases of the classical as well as quantum spin-1/2 system with nearest-neighbour and next-nearest-neighbour isotropic exchange known as the Majumdar-Ghosh Hamiltonian have been extensively studied [33, 34]. Classically, three regimes were identified for $\ell \rightarrow \infty$: ferromagnetic for $J_1 > 0, J_2 > -J_1/4$, antiferromagnetic for $J_1 < 0, J_2 > J_1/4$ and frustrated (spiral) phase otherwise, as the inset to Fig. 1 illustrates. In frustrated phase the pitch angle of the spiral is $\phi = \cos^{-1}(-J_1/4J_2)$ [34]. Quantum fluctuations lower the ground state and shift the phase transition from spin liquid state at $J_2 = 0$ to a dimerized regime with a gap to the excited states at $J_2 = 0.2411J_1$; the transition from antiferromagnetic phase to dimerized singlets takes place at $J_2 = J_1/2$ [33]. In what follows, we elucidate if a polariton linear periodic chain is capable of reproducing the characteristics of classical regimes and what new physics arises due to nonlinear interactions of polaritons.

We plot the values of J_2/J_1 found from Eq. (11) in Fig. 1 and demonstrate that for the experimentally achievable polariton spot widths and wavevectors the values of J_2/J_1 from -0.3 to 0.3 should be realizable. This suggests that all three of the classical regimes, that are depicted in the inset of the Fig. 1, should be accessible in a linear periodic chain.

Next we consider twelve condensates in a linear periodic chain and numerically integrate Eq. (1) for a variety of distances between the spots. For each configuration we start from

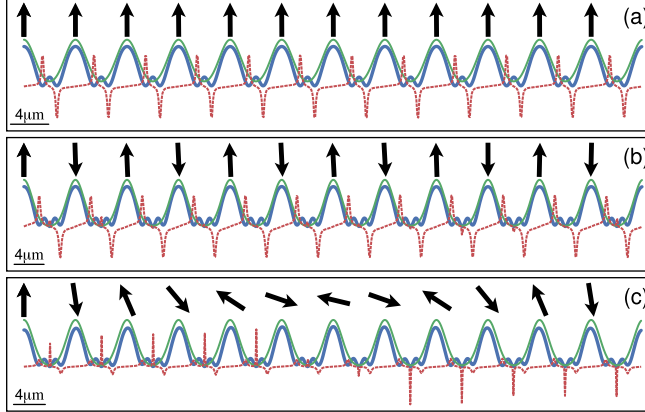


FIG. 2: Polariton densities (blue solid line) and velocities (red dashed lines) for twelve condensates obtained by numerical integration of Eq. (1) with periodical boundary conditions. Pumping profiles are shown with green solid lines. Panel (a) shows the ferromagnetic state, (b) corresponds to antiferromagnetic state with π phase difference between the adjacent sites, and the panel (c) shows the frustrated state. The distances between the nearest condensates are $d = 5.4\mu m$, $d = 6.9\mu m$, and $d = 6.5\mu m$ for (a), (b), and (c), respectively. The numerical parameters for 1D simulations are $\eta = 0.4$, $b = 1.5$, $\gamma = 1$, $p_0 = 5$, $\sigma = 0.4$, $g = 2.5$.

100 random initial distribution of phases to find the ground state configurations. Figure 2 identifies ferromagnetic, antiferromagnetic and spiral spin wave phases that represent the ground states of the one-dimensional XY model. The polariton densities (blue solid lines) are clearly displaced from the pumping profiles (green solid lines) in case of the spin wave state which is depicted in Fig. 2(c). This state has a distinguished velocity pattern (red dashed lines) compared to the other two classical states in Fig. 2(a,b). The experimental systems may suffer from noise, sample disorder, interactions with impurities, so we have repeated the numerical simulations with the Langevin noise described in our previous work [26]. This noise introduces small oscillations around the steady states, but has no effect on the time averaged solutions that coincide with those found without the Langevin noise term.

We have also considered the full two-dimensional system with pumping spots equidistant around a circle. For pumping intensities just above the threshold the same classical phases are obtained. As the pumping intensity increases, the nonlinearity of the system destabilises the frustrated state and produces spin fluctuations, as Fig.3(a-c) illustrates, suggesting the formation of a non-stationary and chaotic spin wave which could be related to phase chaos [35]. Direct observation of non-stationary states in experiments would require time-resolved measurements on time scales that are challenging with current experimental configurations.

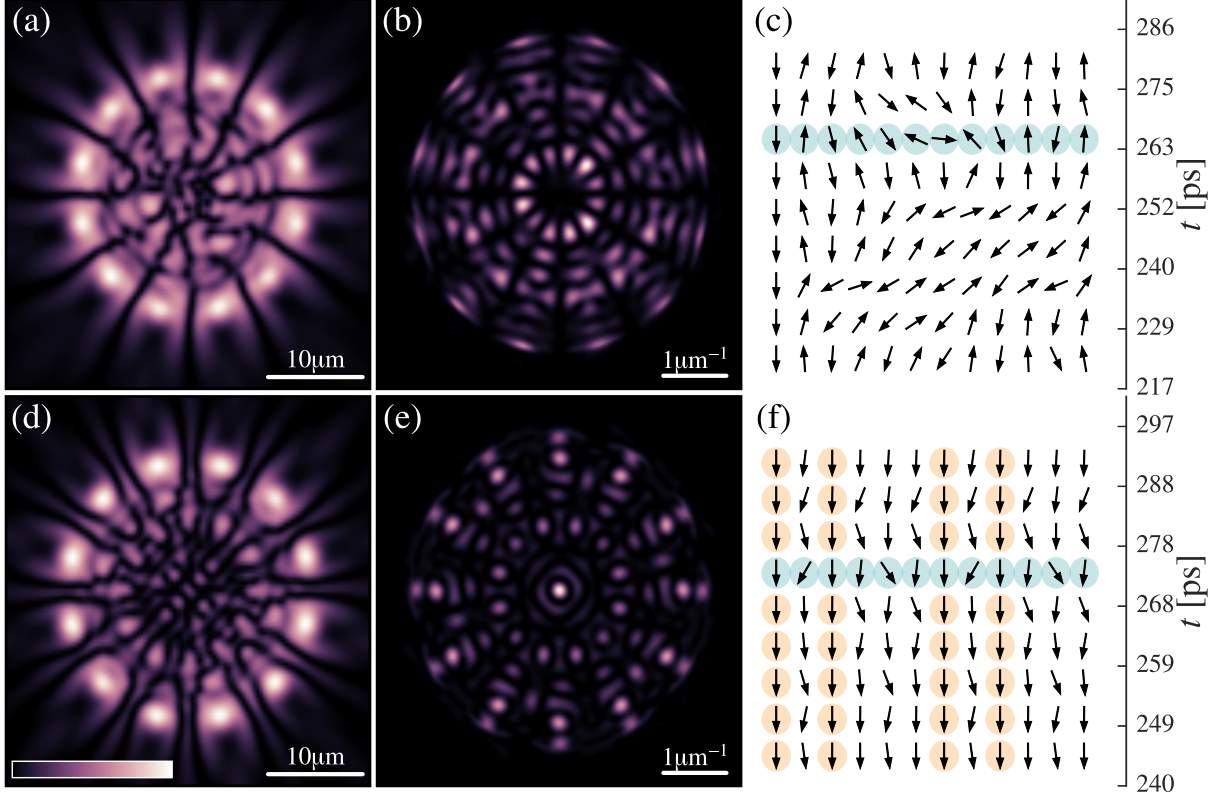


FIG. 3: Density snapshots (left panel) and the far field emission (central panel) at a fixed time for twelve condensates arranged in a circle obtained by numerical integration of Eq. (1). The right panels show the evolution of the phases (relative to one fixed spin) between adjacent spots with $12ps$ (c) and $10ps$ (f) time laps between the spin configurations. The highlighted with blue circles spin configurations in (c) and (f) correspond to the density profiles (a,d) and the far field emissions (b,e). The steady spins of the spots are marked with orange circles in (c,f). We use the simulation parameters that were found to agree with experimental data in our previous works [24?], except for the pumping intensity which is 2.6 times larger to bring about a non-stationary state; the distances between the adjacent sites are $6.4\mu m$ (a-c) and $7\mu m$ (d-f).

Note, that this is the lowest energy state with respect to the XY Hamiltonian, as it carries the largest number of particles for the given network configuration. It suggests that the pumping intensity can be used to continuously move between various state configurations: frustrated states, spin waves, spin liquids, phase chaos etc. and to study transitions between them. For instance, Fig. 3(d-f) demonstrates a non-stationary state of two spin waves of different periods (one or three spins). The spectral weights at a fixed time (Fig. 3(b,e)) reflect the symmetry of the lattice.

Non-stationary spin wave states can be detected in the momentum- and energy-resolved photoluminescence spectrum, which can be directly measured in the far field. Figure 4

shows the spectral weight, $I(\omega, \mathbf{k}) = \left| \iint \Psi(\mathbf{r}, t) \exp[-i\mathbf{k} \cdot \mathbf{r} - i\omega t] dt d\mathbf{r} \right|^2$, as a function of $(\omega, k_x, k_y = 0)$. In the case of the non-stationary state depicted in Fig. 3(a-c), spins reorient themselves randomly with time, cycling through different micro-states with the density distribution depicted in Fig. 4(a). The state shown in Fig. 3(d-f) is a more regular state with the energy spectrum shown in Fig. 4(b) indicating several well separated energy levels. The stationary state would, in contrast, show only one energy level [36, 37].

Frustrated states that we found in the linear periodic chain of polariton graphs correspond to superfluids at nonzero quasi-momentum and, therefore, exhibit nontrivial long range phase order. The spiral phases spontaneously break time-reversal symmetry by generating bosonic currents around the sites of polariton graphs.

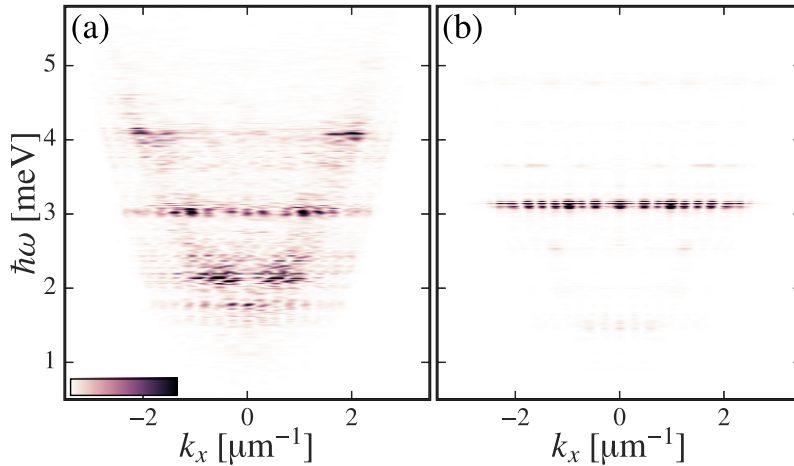


FIG. 4: The spectral weight plots for $k_y = 0$ of the two-dimensional non-stationary spin wave states from Fig. 3(a-c) in (a) and from Fig. 3(d-f) in (b). Both plots are saturated at the same level of 0.2 to make the energy levels more visible and to provide an easier comparison between the states.

In conclusion, we considered polariton condensates arranged in a periodic linear chain. We evaluated the interaction strength between the condensates analytically in terms of the outflow wavevector, pumping width and strength, and the distance between the condensates. We have identified parameter regime where the interactions beyond the next neighbours become important and lead to the appearance of the classical frustrated state. The nonlinear interactions beyond the linear approximation lift the ground state degeneracy and facilitate the formation of a disordered state. We demonstrated that a sequence of polariton condensates are capable of supporting not only classical ground states of the XY model with nearest

and next to nearest neighbour interactions, but also exotic states, such as non-stationary spin waves that may be associated with spin liquids or phase chaos. This observation opens a new path to studying such novel states of matter.

-
- [1] S. Sachdev, Quantum magnetism and criticality, *Nat. Phys.* **4**, 173 (2008).
 - [2] L. Balents, Spin liquids in frustrated magnets, *Nature* **464**, 199 (2010).
 - [3] F. H. L. Essler, H. Frahm, F. Gohmann, A. Klumper, and V. E. Korepin, The one-dimensional Hubbard Model (Cambridge University Press, Cambridge, 2005).
 - [4] A. Auerbach, Interacting electrons and quantum magnetism (Springer, New York, 1994).
 - [5] G. Misguich and C. Lhuillier, Frustrated spin systems, edited by H.T. Diep (World Scientific, Singapore, 2004).
 - [6] F. Alet, A. M. Walczak, and M. P. A. Fisher, Exotic quantum phases and phase transitions in correlated matter, *Physica A* **369(1)**, 122-142 (2006).
 - [7] L. Balents, Spin liquids in frustrated magnets, *Nature* **464**, 199-208 (2010).
 - [8] P. W. Anderson, Resonating valence bonds: A new kind of insulator? *Materials Research Bulletin* **8(2)**, 153-160 (1973).
 - [9] T.-H. Han, J. S. Helton, Sh. Chu, D. G. Nocera, J. A. Rodriguez-Rivera, C. Broholm, and Y. S. Lee, Fractionalized excitations in the spin-liquid state of a kagome-lattice antiferromagnet, *Nature* **492**, 7429 (2012).
 - [10] M. Lewenstein, A. Sanpera, V. Ahufinger, B. Damski, A. Sen, and U. Sen, Ultracold atomic gases in optical lattices: mimicking condensed matter physics and beyond, *Advances in Physics* **56(2)**, 243-379 (2007).
 - [11] M. Saffman, T. G. Walker, and K. Molmer, Quantum information with Rydberg atoms. *Rev. Mod. Phys.* **82**, 2313 (2010).
 - [12] J. Struck, C. Ischlger, R. Le Targat, P. Soltan-Panahi, A. Eckardt, M. Lewenstein, P. Windpassinger, and K. Sengstock, Quantum simulation of frustrated classical magnetism in triangular optical lattices, *Science* **333**, 996 (2011).
 - [13] J. Simon, W. S. Bakr, R. Ma, M. E. Tai, Ph. M. Preiss, and M. Greiner, Quantum simulation of antiferromagnetic spin chains in an optical lattice, *Nature* **472**, 307-312 (2011).
 - [14] J. J. Pla, K.Y. Tan, J. P. Dehollain, W. H. Lim, J. J. L. Morton, F. A. Zwanenburg, D. N.

- Jamieson, A. S. Dzurak, and A. Morello, High-fidelity readout and control of a nuclear spin qubit in silicon, *Nature* **496**, 334-338 (2013).
- [15] R. Hanson and D. D. Awschalom, Coherent manipulation of single spins in semiconductors, *Nature* **453**, 1043-1049 (2008).
- [16] M. Lemesko, N. Y. Yao, A. V. Gorshkov, H. Weimer, S. D. Bennett, T. Momose, and S. Gopalakrishnan, *Phys. Rev. B* **88**, 014426 (2013).
- [17] T. E. Northup and R. Blatt, Quantum information transfer using photons, *Nature Photonics* **8**, 356 (2014).
- [18] B. P. Lanyon, C. Hempel, D. Nigg, M. Müller, R. Gerritsma, F. Zhringer, P. Schindler et al. Universal digital quantum simulation with trapped ions, *Science* **334**, 57 (2011).
- [19] K. Kim, M-S. Chang, S. Korenblit, R. Islam, E. E. Edwards, J. K. Freericks, G-D. Lin, L-M. Duan, and C. Monroe. Quantum simulation of frustrated Ising spins with trapped ions, *Nature* **465**, 590-593 (2010).
- [20] A. D. Corcoles et al. Demonstration of a quantum error detection code using a square lattice of four superconducting qubits, *Nature Commun.* **6**, 6979 (2015).
- [21] S. Utsunomiya, K. Takata and Y. Yamamoto, Mapping of Ising models onto injection-locked laser systems, *Opt. Express* **19**, 18091 (2011).
- [22] A. Marandi, Z. Wang, K. Takata, R. L. Byer, and Y. Yamamoto, Network of time-multiplexed optical parametric oscillators as a coherent Ising machine, *Nature Photonics* **8**, 937-942 (2014).
- [23] M. Nixon, E. Ronen, A. A. Friesem, and N. Davidson, Observing geometric frustration with thousands of coupled lasers, *Phys. Rev. Lett.* **110**, 184102 (2013).
- [24] N. G. Berloff, M. Silva, K. Kalinin, A. Askitopoulos, J. D. Töpfer, P. Cilibrizzi, W. Langbein and P. G. Lagoudakis, Realizing the classical XY Hamiltonian in polariton simulators, *Nature Materials* doi:10.1038/nmat4971 (2017)
- [25] G. Tosi, G. Christmann, N. G. Berloff, P. Tsotsis, T. Gao, Z. Hatzopoulos, P. G. Savvidis, and J. J. Baumberg, Sculpting oscillators with light within a nonlinear quantum fluid, *Nature Physics* **8**, 190-194 (2012).
- [26] H. Ohadi, R. L. Gregory, T. Freearge, Y. G. Rubo, A. V. Kavokin, N. G. Berloff, and P. G. Lagoudakis, Nontrivial Phase Coupling in Polariton Multiplets, *Phys. Rev. X* **6**, 031032 (2016).
- [27] M. Wouters and I. Carusotto, Excitations in a nonequilibrium Bose-Einstein condensate of

- exciton polaritons, *Phys. Rev. Lett.* **99**, 140402 (2007).
- [28] J. Keeling and N. G. Berloff, Spontaneous rotating vortex lattices in a pumped decaying condensate, *Phys. Rev. Lett.* **100**, 250401 (2008).
- [29] P. Cristofolini, A. Dreismann, G. Christmann, G. Franchetti, N.G. Berloff, P. Tsotsis, Z. Hatzopoulos, P.G. Savvidis, J.J. Baumberg, Optical superfluid phase transitions and trapping of polariton condensates, *Physical Review Letters* **110**, 186403 (2013).
- [30] Y. Sun, P. Wen, Y. Yoon, G.Liu, M. Steger, L. N. Pfeiffer, K. West, D. W. Snoke, and K. A. Nelson, *Phys. Rev. Lett.* **118**, 016602 (2017).
- [31] K. Kalinin, M. Silva, W. Langbein, N.G. Berloff, P.G. Lagoudakis, Spontaneous discrete vortex solitons in polariton lattices, submitted to Nature Physics (2017).
- [32] H. Bethe, "Zur Theorie der Metalle. I. Eigenwerte und Eigenfunktionen der linearen Atomkette". (On the theory of metals. I. Eigenvalues and eigenfunctions of the linear atom chain), *Zeitschrift für Physik*, 71:205226 (1931).
- [33] C. K. Majumdar and D. K. Ghosh, *J. Math Phys.* **10**, 1388; **10** 1399, (1969).
- [34] R. Bursill, G. A. Gehring, D. J. J. Farnell, J. B. Parkinson, Tao Xiang, and Chen Zeng, Numerical and approximate analytical results for the frustrated spin-1/2 quantum spin chain, *J. Phys.: Condens. Matter* **7** **45**, 8605-8618 (1995).
- [35] O. V. Popovych, Yu. L. Maistrenko, and P. A. Tass, Phase chaos in coupled oscillators, *Phys. Rev. E* **71**, 065201(R) (2005))
- [36] M. O. Borgh, J. Keeling and N.G. Berloff, Spatial pattern formation and polarization dynamics of a nonequilibrium spinor polariton condensate, *Phys. Rev. B* **81**, 235302, (2010)
- [37] M. O. Borgh, G. Franchetti, J. Keeling and N. G. Berloff, Robustness and observability of rotating vortex-lattices in an exciton-polariton condensate, *Phys. Rev. B* **86**, 035307 (2012)